

This Page Is Inserted by IFW Operations  
and is not a part of the Official Record

## **BEST AVAILABLE IMAGES**

Defective images within this document are accurate representations of the original documents submitted by the applicant.

Defects in the images may include (but are not limited to):

- BLACK BORDERS
- TEXT CUT OFF AT TOP, BOTTOM OR SIDES
- FADED TEXT
- ILLEGIBLE TEXT
- SKEWED/SLANTED IMAGES
- COLORED PHOTOS
- BLACK OR VERY BLACK AND WHITE DARK PHOTOS
- GRAY SCALE DOCUMENTS

**IMAGES ARE BEST AVAILABLE COPY.**

**As rescanning documents *will not* correct images,  
please do not report the images to the  
Image Problem Mailbox.**

(12) INTERNATIONAL APPLICATION PUBLISHED UNDER THE PATENT COOPERATION TREATY (PCT)

(19) World Intellectual Property Organization  
International Bureau



(43) International Publication Date  
6 December 2001 (06.12.2001)

PCT

(10) International Publication Number  
**WO 01/91806 A2**

(51) International Patent Classification<sup>7</sup>: **A61K 51/04**

(21) International Application Number: **PCT/US01/17608**

(22) International Filing Date: **31 May 2001 (31.05.2001)**

(25) Filing Language: **English**

(26) Publication Language: **English**

(30) Priority Data:  
60/208,154 **31 May 2000 (31.05.2000) US**

(71) Applicant (*for all designated States except US*): **STEVEN MCCULLOUGH [US/US]; 5810 Osage Street, Houston, TX 77036 (US).**

(72) Inventors; and

(75) Inventors/Applicants (*for US only*): **WENDT, Richard, E., III [US/US]; 4812 Spruce Street, Bellaire, TX 77401 (US). SIMON, Jaime [US/US]; Route 1, Box 199-A, Angleton, TX 77515 (US).**

(74) Agent: **KARADZIC, Dragan, J.; The Dow Chemical Company, Intellectual Property, B-1211, 2301 N. Brazosport Boulevard, Freeport, TX 77541 (US).**

(81) Designated States (*national*): **AE, AG, AL, AM, AT, AU, AZ, BA, BB, BG, BR, BY, BZ, CA, CH, CN, CO, CR, CZ, DE, DK, DM, DZ, EC, EE, ES, FI, GB, GD, GE, GH, GM, HR, HU, ID, IL, IN, IS, JP, KE, KG, KR, KZ, LC, LK, LR, LS, LT, LU, LV, MA, MD, MG, MK, MN, MW, MX, MZ, NO, NZ, PL, PT, RO, RU, SD, SE, SG, SI, SK, SL, TJ, TM, TR, TT, TZ, UA, UG, US, UZ, YU, ZA, ZW.**

(84) Designated States (*regional*): **ARIPO patent (GH, GM, KE, LS, MW, MZ, SD, SL, SZ, TZ, UG, ZW), Eurasian patent (AM, AZ, BY, KG, KZ, MD, RU, TJ, TM), European patent (AT, BE, CH, CY, DE, DK, ES, FI, FR, GB, GR, IE, IT, LU, MC, NL, PT, SE, TR), OAPI patent (BF, BJ, CF, CG, CI, CM, GA, GN, GW, ML, MR, NE, SN, TD, TG).**

**Published:**

— *without international search report and to be republished upon receipt of that report*

*For two-letter codes and other abbreviations, refer to the "Guidance Notes on Codes and Abbreviations" appearing at the beginning of each regular issue of the PCT Gazette.*

**WO 01/91806 A2**

(54) Title: **A METHOD OF USING A SURROGATE FOR A THERAPEUTIC AGENT TO DETERMINE THE THERAPEUTIC DOSE FOR BONE MARROW ABLATION THERAPY**

(57) Abstract: **A method of using a surrogate, preferably <sup>99m</sup>Tc-MDP, for a therapeutic agent (for example, <sup>166</sup>Ho-EDTMP or preferably <sup>166</sup>Ho-DOTMP) to calculate the dosimetry for the therapeutic dose for bone marrow ablation therapy is disclosed. The advantages of this use of a surrogate *in lieu* of the therapeutic agent is lower cost, less exposure to high radiation levels, and length of the half-life, while maintaining the biodistribution in the total skeleton.**

A METHOD OF USING A SURROGATE FOR A THERAPEUTIC AGENT TO  
DETERMINE THE THERAPEUTIC DOSE FOR BONE MARROW ABLATION  
THERAPY

5           This invention relates to a method of using a tracer  
as a precursor for a therapeutic agent dose for bone  
marrow ablation therapy.

          Several agents that use a radionuclide as the active  
10   component are known or are under development for use in  
treatment of cancer. Some of these agents are especially  
useful for the treatment of calcific tumors. Some of  
these radionuclides are: P-32 and P-33 [see for example,  
Kaplan, E. et al., *J. Nuclear Med.* 1(1), 1, (1960); US  
15   Patent 3,965,254], phosphorus compounds containing boron  
[see for example US Patent 4,399,817], Re-186 [see for  
example Mathieu, L. et al., *Int. J. Applied Rad. &*  
*Isotopes*, 30, 725-727 (1979); Weinenger, J. et al., *J*  
*Nuclear Med.* 24(5), 125 (1983)], Sm-153 [see for example  
20   US Patent 4,898,724], Sr-89 [see for example Firusian, N.  
et al., *J. of Urology*, 116, 764 (1976); Schmidt, C. G. et  
al., *Int. J. Clin. Pharmacol.*, 93, 199-205 (1974)], and  
Ho-166 [see for example, US Patents 5,059,412, 5,006,478,  
and 5,300,279].

25           The reason for such therapeutic agents is to enable  
bone metastases to be treated. Bone metastases are a  
common and often catastrophic event for a cancer patient.  
The pain, pathological fractures, frequent neurological  
30   deficits and forced immobility caused by these metastatic  
lesions significantly decrease the quality of life for the  
cancer patient.

          The use of bone-seeking radiopharmaceuticals for  
35   patient conditioning prior to bone marrow transplantation

(BMT) is a promising approach to increase the delivered radiation dose to the bone marrow above that of conventional total body irradiation (TBI), while maintaining levels that are safe for normal tissues.

5

Therapy for a patient is specific with each treatment based upon a prescribed amount of radioactivity to deliver a calculated radiation absorbed dose to bone marrow [Bayouth, J. E. et al., *Medical Physics* 22(6), 743-753 (1995)]. Control of the amount of radiation for therapy is required to avoid over exposure of radiation to normal tissues and to personnel treating the patient.

Figure 1 shows a graph of biodistribution for comparison between  $^{166}\text{Ho}$ -DOTMP and  $^{99\text{m}}\text{Tc}$ -MDP.

15

Figure 2 shows a graph of lesion to normal bone ratios between  $^{166}\text{Ho}$ -DOTMP and  $^{99\text{m}}\text{Tc}$ -MDP.

Figure 3 is a drawing of a photograph showing the regions used to align the images. The  $^{99\text{m}}\text{Tc}$ -MDP bone scan image (left) is used as the reference image. The body outline of the transmission map (center) is aligned via correlation of its body outline to that of the bone scan, and the  $^{166}\text{Ho}$ -DOTMP image (right) is aligned via maximum correlation of the skeletal image. The skeletal regions described within the specification are delineated by the tetragons.

20

25

Figure 4 shows a graph of the relationship between the value of the scatter multiplier, absolute sensitivity, and mean squared deviation in camera sensitivity.

30

Figure 5 shows a graph of the performance index of the camera/collimator combination as a function of the scatter multiplier value.

35

Figure 6A shows a graph of the comparison of the calculated vs. measured attenuation correction factor (ACF) relationship between the 80 keV photons of  $^{166}\text{Ho}$  and the 122 keV photons of  $^{57}\text{Co}$  in simulated tissue (acrylic).

5

Figure 6B shows a graph of the calculated vs. measured ACF relationship between the 50 keV photons of  $^{166}\text{Ho}$  and the 122 keV photons of  $^{57}\text{Co}$  in simulated tissue (acrylic).

10

Figure 7 shows a graph of the comparison of relative skeletal biodistribution of  $^{166}\text{Ho}$ -DOTMP and its surrogate,  $^{99\text{m}}\text{Tc}$ -MDP. The fraction of total skeletal content of  $^{166}\text{Ho}$ -DOTMP for various skeletal regions was compared to the same region with  $^{99\text{m}}\text{Tc}$ -MDP for every patient.

15

Figure 8 shows a graph illustrating the relative skeletal biodistribution of  $^{166}\text{Ho}$ -DOTMP and  $^{99\text{m}}\text{Tc}$ -MDP.

20

Figure 9 shows a graph of the results of absolute skeletal uptake measurements for each radiopharmaceutical agent. Values represent the measured percent localization of each radiopharmaceutical agent in the skeleton at late time points (>18 hours post injection).

25

Figure 10 shows a graph of the total skeletal residence times calculated for individual patients comprising results obtained with a tracer study of  $^{166}\text{Ho}$ -DOTMP and a surrogate study using  $^{99\text{m}}\text{Tc}$ -MDP.

30

This invention relates to a method of therapeutic treatment for bone marrow ablation of a patient using radiopharmaceuticals which comprises using a first radiopharmaceutical agent as a surrogate for the therapeutic second radiopharmaceutical agent, while having total skeletal uptake with similar skeletal residence

35

time, to determine dosimetry prior to administering the therapeutic dose to the patient of the therapeutic second radiopharmaceutical agent.

5       The bone-seeking chelating agent used for bone marrow ablation may be selected from 1,4,7,10-tetraazacyclododecane-1,4,7,10-tetramethylenephosphonic acid (DOTMP) or ethylenediaminetetramethylenephosphonic acid (EDTMP), with DOTMP being preferred. Holmium-166 was  
10 chosen as the isotope since it emits a high energy beta (1.84 MeV E<sub>max</sub>) required for therapy and has a relatively short half-life (26.8 hours), thereby allowing a relatively short interval to transplantation. Holmium-166 also has a small proportion of low energy photons (80 and  
15 50 keV) that are suitable for radionuclide imaging, but do not pose a significant radiation hazard. Holmium-166 1,4,7,10-tetraazacyclododecane-1,4,7,10-tetramethylenephosphonic acid (<sup>166</sup>Ho-DOTMP) is a bone  
20 seeking radiopharmaceutical agent that is useful for bone marrow ablation.

When high activity is required for use of these agents (1 Ci or more total administered radioactivity), it is important to understand where they localize and  
25 determine dosimetry information (organ scale dosimetry or MIRD, sub-organ scale skeletal dosimetry, and image based dosimetry) prior to administration of these drugs. The most widely accepted method for internal d is that developed by the Medical Internal Radiation Dose Committee  
30 of the Society of Nuclear Medicine (MIRD) [Loevinger, R. L. et al., MIRD Primer for Absorbed Dose Calculations, NY, Society of Nuclear Medicine (1991)]. In utilizing the MIRD methodology for bone-seeking radiopharmaceuticals the only patient specific variable is the cumulative number of  
35 radioactive decays occurring within the skeleton (residence time). The distribution of radioactivity

within the skeleton is assumed to be uniform, which is incorrect for  $^{166}\text{Ho}$ -DOTMP [Bayouth, J. E. et al., *Medical Physics* 22(6), 743-753 (1995)]. More accurate dosimetry would incorporate variations in the radiopharmaceutical distribution within the skeleton.

The scale of skeletal dosimetry calculations is limited by the ability to resolve the localization of the radioisotope within the skeleton. Holmium-166 does not usually provide high resolution nuclear imaging so that technetium-99m was used as an alternative because of its better resolution nuclear image, relatively inexpensive, and commercially available.

$^{166}\text{Ho}$ -DOTMP is a known therapeutic agent for use in bone marrow ablation (see US Patent 5,509,412).  $^{99\text{m}}\text{Tc}$ -MDP is a known, commercial diagnostic reagent (available from Squibb, Mallinckrodt, CIS/US, DuPont Medipysics, and Merck Frost and is a standard imaging radiopharmaceutical for bone imaging in nuclear medicine.

$^{166}\text{Ho}$ -DOTMP is being evaluated for use in bone marrow ablation. Because patients have variable skeletal uptake of  $^{166}\text{Ho}$ -DOTMP, a diagnostic dose of  $^{166}\text{Ho}$ -DOTMP is used to determine the uptake for each patient to calculate the therapeutic dose. However, the  $^{166}\text{Ho}$ -DOTMP diagnostic dose is quite expensive to make and has a short shelf life. Thus a suitable surrogate tracer complex which has an uptake mechanism similar to  $^{166}\text{Ho}$ -DOTMP could be used to determine this therapeutic dose such that absolute skeletal uptake can be measured as well as the localization and pharmacokinetics. Also such a tracer could enable patients to be screened for uptake of the tracer to determine whether a therapeutic dose of  $^{166}\text{Ho}$ -DOTMP should be administered.

Due to the high level of activity (frequently between about 1 and about 4 Ci total administered dosage) required for using a radionuclide agent, preferably Ho-166 in a complex (such as holmium-166 1,4,7,10-tetraazacyclododecane-1,4,7,10-tetramethylenephosphonic acid or  $^{166}\text{Ho}$ -DOTMP), a tracer is desired to determine the dose of the  $^{166}\text{Ho}$ -DOTMP to administer. The use of such a tracer avoids more agent being administered than required for treatment to the patient and lowers the exposure level to radiation of the personnel administering the agent. Because the agent is quite expensive, has a short half-life (about 27 hours), and does not image very well (gamma photons of 50 and 80 keV), a tracer that is inexpensive, and delivers significantly less radiation dose to the patient than the agent is desired. This invention concerns the use of technetium-99m methylenediphosphonic acid or  $^{99\text{m}}\text{Tc}$ -MDP as the tracer for the agent  $^{166}\text{Ho}$ -DOTMP.

For therapeutic doses of radio-pharmaceuticals is it usual to give a preparative dose to determine the dosimetry and calculate the therapeutic dose using the desired therapeutic agent. However, it is not easy to obtain the biodistribution for  $^{166}\text{Ho}$ -DOTMP because of its relatively poor imaging characteristics. Also the agent is relatively expensive to prepare and with its short half-life must be used promptly after preparation. Therefore indirect distribution assessment was done using  $^{99\text{m}}\text{Tc}$ -MDP as the tracer. Even though the half-life of  $^{99\text{m}}\text{Tc}$  is shorter (16.02 hours), it is readily available and much less expensive to produce. This tracer has superior imaging with a similar uptake in the bone compared to  $^{166}\text{Ho}$ -DOTMP. This tracer has been confirmed as valuable for this purpose by comparison of DOTMP and MDP in gross skeletal distribution and by comparison of lesion to normal bone ratios.



An attenuation correction for both radionuclides was performed using transmission-emission techniques with either a  $^{57}\text{Co}$  sheet source or  $^{99\text{m}}\text{Tc}$  line source as the transmission source. A correction from 122/140 keV to 49, 81 and 140 keV was determined experimentally. The biodistribution in the skeleton was then determined by subdividing the skeleton by a standard method using anatomical landmarks to identify region borders and comparing attenuation corrected activity distribution. (See Figure 1.)

In addition to providing higher resolution surrogate images for estimating the  $^{166}\text{Ho}$ -DOTMP biodistribution, the  $^{99\text{m}}\text{Tc}$ -MDP could also provide a cost-effective alternative for determining skeletal residence time necessary for patient specific dosimetry. Due to the heterogeneity in initial skeletal uptake among patients treated with  $^{166}\text{Ho}$ -DOTMP, patient-specific pharmacokinetic measurements are required for  $^{166}\text{Ho}$ -DOTMP treatment planning [Bayouth, J. E., Radiation Physics. Houston, University of Texas, Houston Graduate School of Biomedical Science: 111 (1993)]. The measurements are usually obtained over a 48 hour period following a tracer injection of about 30 mCi. Whole body imaging has demonstrated that mostly skeletal activity is present at times greater than 18 hours post injection (<5% of the injected  $^{166}\text{Ho}$ -DOTMP or  $^{99\text{m}}\text{Tc}$ -MDP dose is found within the soft tissue). Those late whole body retention curves are used to extrapolate the initial skeletal uptake. If  $^{99\text{m}}\text{Tc}$ -MDP could accurately predict the skeletal uptake of  $^{166}\text{Ho}$ -DOTMP, it would provide an inexpensive and widely available method for screening patient eligibility and obtaining initial dosimetry planning data.

$^{99\text{m}}\text{Tc}$ -MDP provides a lower cost, higher quality image, and alternative method for preliminary estimation of  $^{166}\text{Ho}$ -

DOTMP biodistribution and absolute uptake to determine the therapeutic dose.

Theory of the Invention

5

While not wishing to be bound by theory, it is believed that the advantageous results of the present invention are obtained because of similarity of biodistribution between  $^{99m}\text{Tc}$ -MDP and  $^{166}\text{Ho}$ -DOTMP because of  
10 the mechanism of binding to the bone of these two complexes. It is believed that other known bone ligands (for example, ethylenediaminetetramethylenephosphonic acid complexed to  $^{166}\text{Ho}$ ) may perform in a similar manner.

15 In the standard method of administering a radiopharmaceutical agent, a dose of agent is given to a patient to determine the dosimetry of the agent prior to the actual administration to the patient of the therapeutic dose of the agent. To ensure that the  
20 biodistribution is the same, the same agent is used. In contrast to this standard practice, this invention provides a method for using a surrogate tracer  $^{99m}\text{Tc}$ -MDP for the usual dose for dosimetry of the therapeutic agent  $^{166}\text{Ho}$ -DOTMP. The biodistribution of the two agents are  
25 sufficiently similar to permit the required calculations for the therapeutic dose of the agent. The reasons that this invention is useful for this particular therapeutic agent is that the agent is quite expensive to use for such a dosimetry dose, the short half-life of the agent and the  
30 difficulty of producing it limits its availability, and the total skeletal uptake of the agent is required. The present surrogate agent provides estimates of this total skeletal uptake with an accuracy of  $\pm 10\%$  and the total skeletal residence time with an accuracy of  $\pm 13\%$ , assuming  
35 a fixed biological clearance rate for the therapeutic agent from the skeleton. These values translate directly

to a maximum of  $\pm 13\%$  error in the prescribed  $^{166}\text{Ho}$ -DOTMP activity required for therapy or the total delivered marrow dose. Uncertainties in the radionuclide dosimetry can exceed 25% for normal organs and well-modeled  
5 pharmaceuticals and may be much larger in tumors or organs significantly altered by disease [Fisher, D. *Cancer*, 73(3 Suppl.), 905-11 (1994)]. Thus this invention falls within the errors of conventional internal dosimetry.

## 10 Experimental and Discussion

The invention will be further clarified by a consideration of the following examples, which are intended to be purely exemplary of the present invention.

15

As shown by the following examples, statistical analysis demonstrated excellent linear correlation of  $^{99\text{m}}\text{Tc}$ -MDP and  $^{166}\text{Ho}$ -DOTMP for absolute uptake at late time points ( $>18$  hours post injection) ( $r^2=0.94$ ) and gross  
20 skeletal biodistribution ( $r^2=0.96$ ).  $^{99\text{m}}\text{Tc}$ -MDP was able to accurately predict the skeletal residence time for  $^{166}\text{Ho}$ -DOTMP within 13% of the measured value in all twenty patients evaluated. Evaluation of the relationship between  $^{99\text{m}}\text{Tc}$ -MDP and  $^{166}\text{Ho}$ -DOTMP skeletal biodistribution  
25 and absolute skeletal uptake was performed.

In imaging of the patient with  $^{166}\text{Ho}$ -DOTMP multiple energy windows (20% scatter window at 100 keV (US), 20% photopeak window at 80 keV, 15% scatter window at 59 keV  
30 (LS), and 15% photopeak window at 50 keV) were used. The benefits of multiple energy windows are: (a) there is a higher signal-to-noise ratio in the final image (which compensates for the low photon yield and poor count for  $^{166}\text{Ho}$  and that the fraction counts from the background or  
35 scatter is significant); and (b) scatter correction of photopeak images is possible (thus triple energy window

corrects for the 81 keV photopeak images and dual energy window correction for the 49 keV photopeak images).

Image analysis is done by a semi-automatic procedure  
5 where Interfile-formatted images are read in, orientated,  
and appropriate manipulations applied. The images are  
grossly aligned using maximum correlation method over both  
x and y shifts. Body contour is used to register  
transmission image to the  $^{99m}\text{Tc}$ -MDP image. The emission  
10 images are registered by weighing the correction by the  
pixel values. The images of the skeleton are effectively  
dismembered at joints. These images are then registered  
via correlation allowing for both translation and  
rotation. Attenuation correction is then directly applied  
15 to each anatomical section. Binary masks obtained from  
thresholding each section are applied. Total counts in  
each region are calculated. Statistical analysis  
demonstrated excellent linear correlation of  $^{99m}\text{Tc}$ -MDP and  
 $^{166}\text{Ho}$ -DOTMP for absolute uptake at late time points (>18  
20 hours post injection) ( $r^2=0.94$ ) and gross skeletal  
biodistribution ( $r^2=0.96$ ).  $^{99m}\text{Tc}$ -MDP was able to accurately  
predict the skeletal residence time for  $^{166}\text{Ho}$ -DOTMP within  
13% of the measured value. From these studies it has been  
shown that intraskeletal biodistribution of  $^{99m}\text{Tc}$ -MDP  
25 closely mimics  $^{166}\text{Ho}$ -DOTMP and that  $^{166}\text{Ho}$ -DOTMP may have a  
higher affinity for osteoblastic lesions than  $^{99m}\text{Tc}$ -MDP.  
(See Figure 2.)

#### Working Examples

30

##### Example 1

Twenty-two patients (18 multiple myeloma patients and  
4 patients with breast cancer metastatic to bone) received a  
transmission scan using a Co-57 sheet source for  
35 transmission-emission attenuation correction.  
Reproducible positioning was accomplished through the use

of immobilizing "bean bag" type cushions commonly used in radiotherapy (Vac-Loc 100x200 cm, MED-TEC Inc., Orange City, IA). Photon attenuation for these bags at 122 keV was measured to be less than 0.1%.

5

Quantitative whole body bone scans (30 mCi injection  $^{99m}\text{Tc}$ -MDP) were acquired for each patient at 0, 4, and 20 hours after injection on a dual headed gamma camera (BIAD, Trionix Labs, OH). The camera sweep rate was set at the maximum speed for the initial image (>28 cm/min) and slowed to the minimum speed for the remaining images (<7.5 cm/min). All  $^{99m}\text{Tc}$  camera images were acquired with single 20% wide energy windows centered around 140 keV. Two imaging standards were included in each image: one in air and the other inside a 20 cm thick acrylic block simulating tissue (Dual Source Scatter Phantom, Nuclear Associates, Carle Place, NY). Following a waiting period of 4 days, the study was repeated with 30 mCi of  $^{166}\text{Ho}$ -DOTMP. Post injection scans were acquired at the same times and same sweep rates as the prior bone scans.

Due to the mixed photon spectrum and bremsstrahlung production of  $^{166}\text{Ho}$ -DOTMP (Table 1 below), all images must be corrected for scattered radiation and collimator spatial penetration. Four energy windows were utilized: two photopeak windows and two scatter windows each placed above and adjacent to the corresponding photopeak windows. Energies and window widths were: 20% wide at 80 keV and 15% wide at 50 keV. Scatter windows had the same widths as the corresponding photopeak. After acquisition the windows were combined in a linear fashion as follows: scatter corrected image = photopeak image - K\* scatter image where K is the scatter multiplier.

Scatter multipliers ( $K_{80}$  and  $K_{50}$ ) for  $^{166}\text{Ho}$  were determined experimentally with the goal to minimize the

deviation of camera sensitivity for sources of varying activity, depth in tissue, and source to collimator distance, while maintaining adequate sensitivity.

5           **Table 1**

Relative photon abundance for  $^{166}\text{Ho}$ .

Beta particle and resultant bremsstrahlung emissions are not included

Emission	% Abundance	Energy (keV)
Gamma	6.71	80.5
Gamma	0.02	674
Gamma	0.01	705
Gamma	0.01	786
Gamma	0.93	1379
Gamma	0.19	1582
Gamma	0.12	1662
Gamma	0.03	1750
Gamma	0.01	1830
X-ray	5.50	49
X-ray	3.10	48
X-ray	2.25	55

10           Images were acquired of a phantom filled with  $^{166}\text{Ho}$ -  
 DOTMP that was constructed to simulate various sources of  
 uniform activity and variable source area. Source-to-  
 collimator distance (STC) dependence was evaluated for  
 medium energy collimators on a dual headed gamma camera  
 15 (BIAD, Trionix Research Laboratory, Twinsberg, OH) at  
 several distances from the collimator. Medium energy  
 collimators were previously shown to provide the highest  
 sensitivity for  $^{166}\text{Ho}$ -DOTMP while still maintaining  
 adequate shielding against higher energy photons [Bayouth,  
 20 J. E., Radiation Physics. Houston, University of Texas,  
 Houston Graduate School of Biomedical Science: 111  
 (1993)].

Following the STC distance experiment, the phantom was placed at a fixed distance (20 cm) from the collimator surface and successive images were acquired with increasing thickness of acrylic placed on either side of the phantom to simulate tissue. The mean square deviation in the camera sensitivity as a function of STC distance, depth in simulated tissue, and source size were calculated. For each possible value of the scatter multipliers, the ratio of camera sensitivity to mean square deviation was evaluated. The value of the scatter multiplier corresponding to the maximum value of the sensitivity to deviation ratio was chosen, providing the greatest sensitivity with the smallest amount of error.

15

Following scatter correction, proper attenuation correction was required. The transmission-emission technique was chosen for attenuation correction, however, since the transmission and emission isotopes differed, the relationship between the attenuation correction factors (ACFs) for the different isotopes were established. The previously described phantom was used for this experiment. Each region within the phantom was again filled with the radioactive solution of uniform activity concentration. The phantom was entered with a total separation of 40 cm between the two camera heads using medium energy collimators. Images were acquired with increasing thickness of acrylic scatter material placed on either side of the phantom (0, 3.6, 7.2, 14.4, and 21.8 cm total thickness). Measured ACF values were averaged over the various sized sources in the phantom following proper scatter subtraction using previously determined scatter multipliers. ACF values for Co-57 were acquired in an identical manner for the same total thickness of acrylic. Simple exponential attenuation suggests that a power relationship should exist between two ACFs where the power

exponent is the ratio of the two attenuation coefficients for the two energy photons. With each data set acquired, the best fit power relationship between Co-57 and the isotope of interest was determined using least squared regression techniques.

### Example 2

The biodistribution of each radiopharmaceutical was evaluated in acquired patients' images to compare skeletal localization of  $^{99m}\text{Tc}$ -MDP and  $^{166}\text{Ho}$ -DOTMP. The goal was to measure the fraction of the radio-pharmaceutical ( $^{166}\text{Ho}$ -DOTMP) that localized in a given anatomical region of the skeleton and to compare that fraction to that of the surrogate material ( $^{99m}\text{Tc}$ -MDP) at the same time point. The individual regions were taken as those anatomical regions defined in the bone/bone marrow dosimetry model in the MIRDose 3.1 software package with some combining of overlying regions: skull (cranium + facial + C1-C5), spinal column [middle (C6, C7 + all thoracic) + sternum], lower spine (L1-L4), chest cage (right ribs + left ribs + scapulae + clavicles), pelvis + L5 + femoral heads, upper and lower legs, and upper and lower arms [Eckerman, K and M. Stabin, *J. Nuclear Med.*, 35, 112 (1994)].

The initial registration of the transmission and emission images was very good due to the use of immobilization devices, however, further registration of the images was necessary. While the whole skeleton is not a rigid body, the various regions described previously can be considered rigid structures requiring only translation and rotation to align. The  $^{99m}\text{Tc}$ -MDP image was chosen as the reference image to align to because it is easy to discern both the skeleton and the body outline on one image. The body outline is used to align the transmission image, while the skeleton is used to register the  $^{166}\text{Ho}$  image (see Figure 3). Registration is achieved by



searching for the maximum correlation of the two images within a given range of translation and rotation values. With all three images aligned, the attenuation correction map is then applied to each region and the total number of counts recorded. This procedure was repeated for each region of the skeleton and the results compiled for all patients.

### Example 3

Current dosimetry models calculate the radiation absorbed dose delivered to the target organ based upon an assumed homogeneous distribution of the radiopharmaceutical in the source organ. The estimated marrow absorbed dose from activity localized within the skeleton is directly proportional to the total residence time within the skeleton. For all patients studied, the whole body pharmacokinetics for  $^{166}\text{Ho}$ -DOTMP were measured via serial imaging, serial whole body probe measurements, and cumulative urine measurements [Bayouth, J. E., Radiation Physics. Houston, University of Texas - Houston Graduate School of Biomedical Science: 111 (1993)].  $^{99\text{m}}\text{Tc}$ -MDP pharmacokinetics were measured from serial whole body imaging only. A quick whole body sweep ( $>28$  cm/min) was acquired immediately following injection to serve as the 100% point, and all subsequent images were acquired at a slower rate ( $<7.5$  cm/min). All images contained standards for normalization: one in air and the other placed in the center of a 20 cm thick block of acrylic. Little or no  $^{99\text{m}}\text{Tc}$ -MDP or  $^{166}\text{Ho}$ -DOTMP radioactivity can be found within the soft tissues after 18 hours post-injection. The percentage of initial  $^{99\text{m}}\text{Tc}$ -MDP activity remaining in the whole body (skeleton) at the late scan time ( $>18$  post injection) was then compared to that for  $^{166}\text{Ho}$ -DOTMP at the same time post-injection.

35

Example 4

The deviation in sensitivity of the camera to sources of the various size, activity, and STC distance were evaluated for all practical values of the scatter multipliers (see Figure 4). A decline in camera sensitivity was experienced as the scatter multiplier was increased. The ratio of those two functions reached a maximum at the optimal value of the scatter multiplier (see Figure 5). The optimal values of the scatter multipliers are shown in Table 2 below. The set of values for the 80 keV peak agree well with previously determined values using high energy collimators [Bayouth, J. E., Radiation Physics. Houston, University of Texas, Houston Graduate School of Biomedical Science: 111 (1993)] and properly returned areas with no activity to near zero counts.

**Table 2**

Optimal values for  $^{166}\text{Ho}$  scatter multipliers calculated for medium energy collimators on a Trionix BIAD camera system.

Scatter Multiplier	Optimal Value for Medium Energy Collimators	Optimal Value for High Energy Collimators <sup>a</sup>
$K_{80}$ (80 keV- $K1*US^b$ )	1.0	1.0
$K_{50}$ (50 keV - $K2*LS^c$ )	0.65	n/a

a = Previously determined values for high energy collimators are also included. Bayouth, J. E., Radiation Physics. Houston, University of Texas, Houston Graduate School of Biomedical Science: 111 (1993)

b = upper scatter

c = lower scatter

n/a = not available

Example 5

Measured ACF data were compared to simple exponential attenuation calculations. Due to buildup processes, this agreement of the theoretical and measured data is not good, but is still adequate to calculate a relationship between the ACF for  $^{166}\text{Ho}$  and  $^{57}\text{Co}$ . Simple exponential attenuation suggests that a power relationship should exist where the exponent is the ratio of the two attenuation coefficients. The measured and theoretical relationships of the ACFs for  $^{166}\text{Ho}$  (80 and 50 keV),  $^{99\text{m}}\text{Tc}$  and  $^{57}\text{Co}$  are summarized in Table 3 below. A comparison of the measured and calculated ACF relationship between both the 80 keV and 50 keV photons of  $^{166}\text{Ho}$  and 122 keV photons of  $^{57}\text{Co}$  are shown in Figures 6A and 6B. Error bars represent two standard deviations of the mean ACF calculated from five sources of various source strength and size. Similar experiments were performed to relate  $^{99\text{m}}\text{Tc}$  and  $^{57}\text{Co}$ .

Table 3

Calculated and measured parameters relating the attenuation correction coefficients of  $^{166}\text{Ho}$  (80 and 50 keV) to that of  $^{57}\text{Co}$

ACF Values	Calculated Relationship	Actual Measured Relationship
$^{57}\text{Co}$ & $^{166}\text{Ho}$ (80 keV)	$\text{ACF}_{\text{Ho}(80)} = (\text{ACF}_{\text{Co}})^{1.12}$	$\text{ACF}_{\text{Ho}(80)} = (\text{ACF}_{\text{Co}})^{1.48}$
$^{57}\text{Co}$ & $^{166}\text{Ho}$ (50 keV)	$\text{ACF}_{\text{Ho}(50)} = (\text{ACF}_{\text{Co}})^{1.33}$	$\text{ACF}_{\text{Ho}(50)} = (\text{ACF}_{\text{Co}})^{1.61}$
$^{57}\text{Co}$ & $^{99\text{m}}\text{Tc}$	$\text{ACF}_{\text{Tc}} = (\text{ACF}_{\text{Co}})^{0.96}$	$\text{ACF}_{\text{Tc}} = (\text{ACF}_{\text{Co}})^{1.2}$

25

A comparison of the relative skeletal biodistribution shows good correlation between  $^{99\text{m}}\text{Tc}$ -MDP and  $^{166}\text{Ho}$ -DOTMP (see Figure 7). While there are significant differences in the distributions among individual patients, the agreement between the two agents is very good with the regression

30

relationship being 1:1. Relative distribution data (see Figure 8) shows that the vast majority of the radioactivity is concentrated in the axial skeleton (chest cage, spine, head and pelvis) with good agreement between  $^{166}\text{Ho}$ -DOTMP and  $^{99\text{m}}\text{Tc}$ -MDP.

#### Example 6

While the initial skeletal uptake of  $^{166}\text{Ho}$ -DOTMP can vary significantly from patient to patient, the rate of clearance from the skeleton appears to be relatively constant (see Table 4 below). Therefore, the single most important factor in determining the residence time of  $^{166}\text{Ho}$ -DOTMP in the skeleton is the estimated uptake within the skeleton.

Table 4

Summary of measured skeletal pharmacokinetic parameters for  $^{166}\text{Ho}$ -DOTMP in 20 patients.

Parameter	Mean	Standard Deviation	Range
Fractional Skeletal Uptake (%)	26	10	15-55
Effective Half-life (hours)	20.5	1.7	18-24

This data suggests that the rate of clearance from the skeleton is relatively constant, while absolute uptake varies significantly.

By assuming a rate of clearance this can be easily determined from the fraction of activity residing in the whole body at times greater than 18 hours after injection. Pharmacokinetics appear similar for both pharmaceutical agents. For all patients, the absolute skeletal uptake of

<sup>99m</sup>Tc-MDP is higher than that of <sup>166</sup>Ho-DOTMP, however, there is excellent linear correlation between the uptake of the two agents at times greater than 18 hours post injection. Figure 9 illustrates the relationship between the  
5 estimated skeletal uptake of the two agents measured via the whole body retention at 18 to 22 hours post injection. The equation that best describes the skeletal uptake relationship between the two pharmaceuticals is:

10 
$$\% \text{Uptake } ^{166}\text{Ho-DOTMP} = 0.85 * (\% \text{Uptake } ^{99m}\text{Tc-MDP}) - 7.3\%$$

Two outliers were noted (both were administered a different brand and formulation of <sup>99m</sup>Tc-MDP bone scanning agent which resulted in significantly lower <sup>99m</sup>Tc-MDP  
15 uptake and clinically detectable loss of bone to soft tissue contrast in the image). For both of these patients, the absolute uptake of each agent was approximately equal.

20 Example 7

A final test for this method was to estimate the skeletal residence time using the surrogate data with an assumed clearance of 20.5 hours and to compare to the calculated skeletal residence time from the <sup>166</sup>Ho-DOTMP  
25 tracer study (see Figure 10). Total skeletal residence times, as estimated from the <sup>99m</sup>Tc-MDP were within  $\pm 9\%$  of the values determined from <sup>166</sup>Ho-DOTMP for 17 of the 20 patients studied and within  $\pm 13\%$  for all patients studied.

30 Although the invention has been described with reference to its preferred embodiments, those of ordinary skill in the art may, upon reading and understanding this disclosure, appreciate changes and modifications which may be made which do not depart from the scope and spirit of  
35 the invention as described above or claimed hereafter.

## WHAT IS CLAIMED IS:

1. A method of therapeutic treatment for bone marrow ablation of a patient using radiopharmaceuticals which  
5 comprises using a first radiopharmaceutical agent as a surrogate for the therapeutic second radiopharmaceutical agent, while having total skeletal uptake with similar skeletal residence time, to determine dosimetry prior to administering the therapeutic dose to the patient of the  
10 therapeutic second radiopharmaceutical agent.
2. A method of Claim 1 further comprising that the first radiopharmaceutical agent display similar biodistribution to that of the therapeutic second radiopharmaceutical  
15 agent.
3. The method of Claim 1 wherein the first radiopharmaceutical agent comprises technetium-99m methylenediphosphonic acid.  
20
4. The method of Claim 1 wherein the therapeutic second radiopharmaceutical agent comprises holmium-166 1,4,7,10-tetraazacyclododecane-1,4,7,10-tetramethylenephosphonic acid or holmium-166 ethylenediaminetetramethylene-  
25 phosphonic acid.
5. The method of Claim 1 wherein the first radiopharmaceutical agent comprises technetium-99m methylenediphosphonic acid and the therapeutic second  
30 radiopharmaceutical agent is holmium-166 1,4,7,10-tetraaza-cyclododecane-1,4,7,10-tetramethylene-phosphonic acid.
6. The method of Claim 1 wherein the first  
35 radiopharmaceutical agent provides estimates of the total skeletal uptake with an accuracy of  $\pm 10\%$ .

7. The method of Claim 1 wherein the total skeletal residence time can provide estimates with an accuracy of  $\pm 13\%$ , assuming a fixed biological clearance rate for the therapeutic agent from the skeleton.
- 5
8. The method of Claim 1 wherein the therapeutic dose is between about 1 and about 4 Ci total administered dosage.

FIG. 1

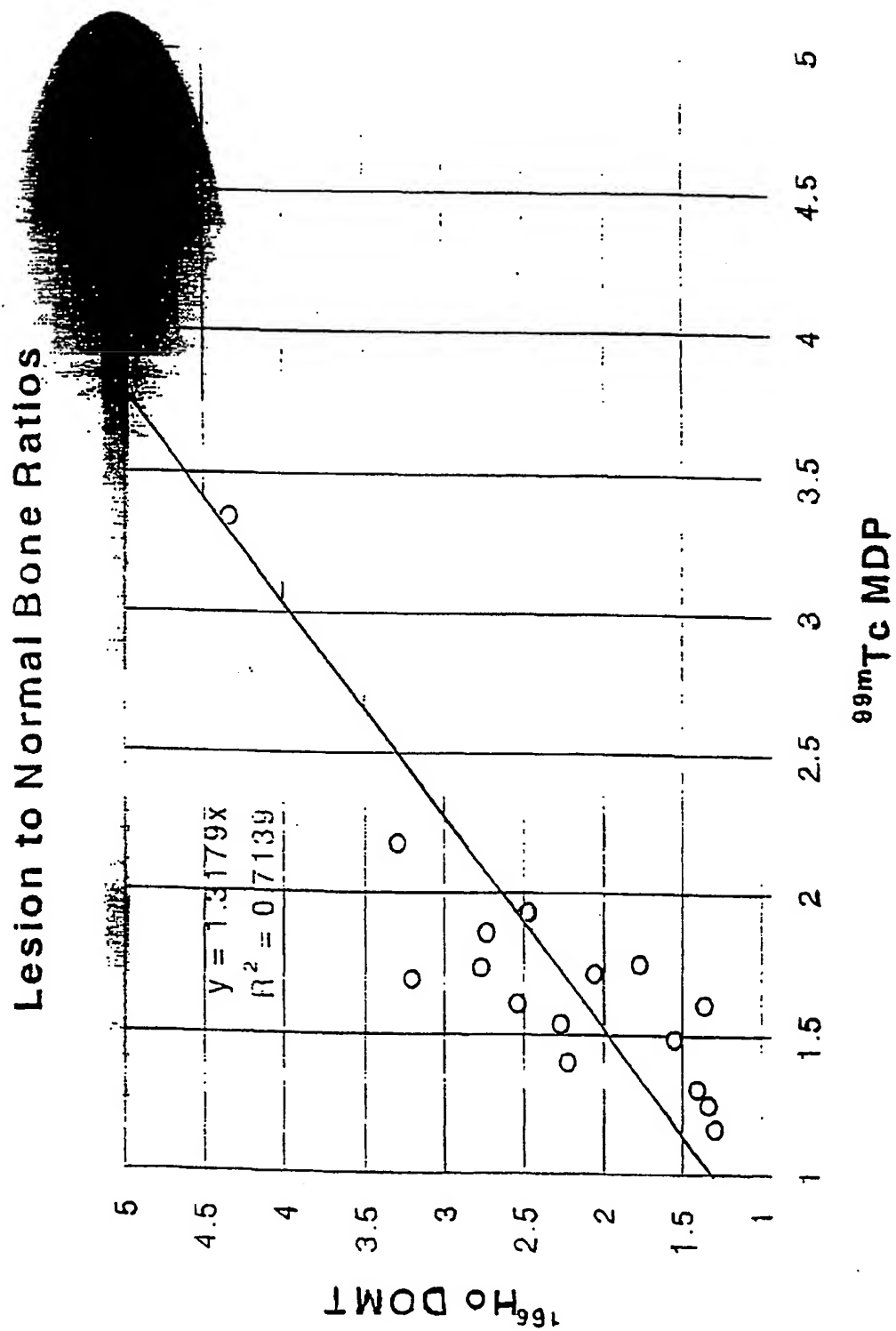
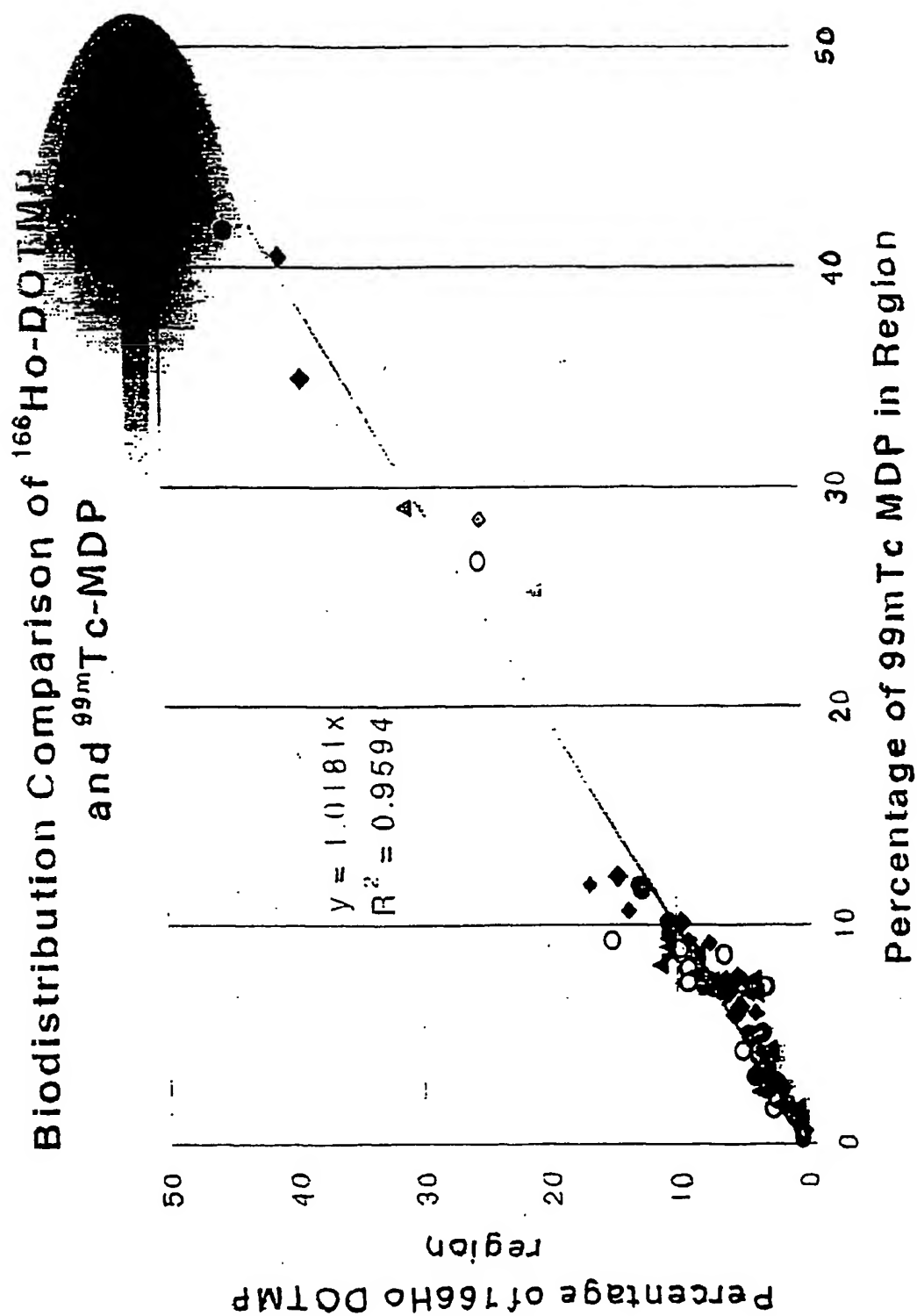




FIG. 2



3/11

FIG. 3

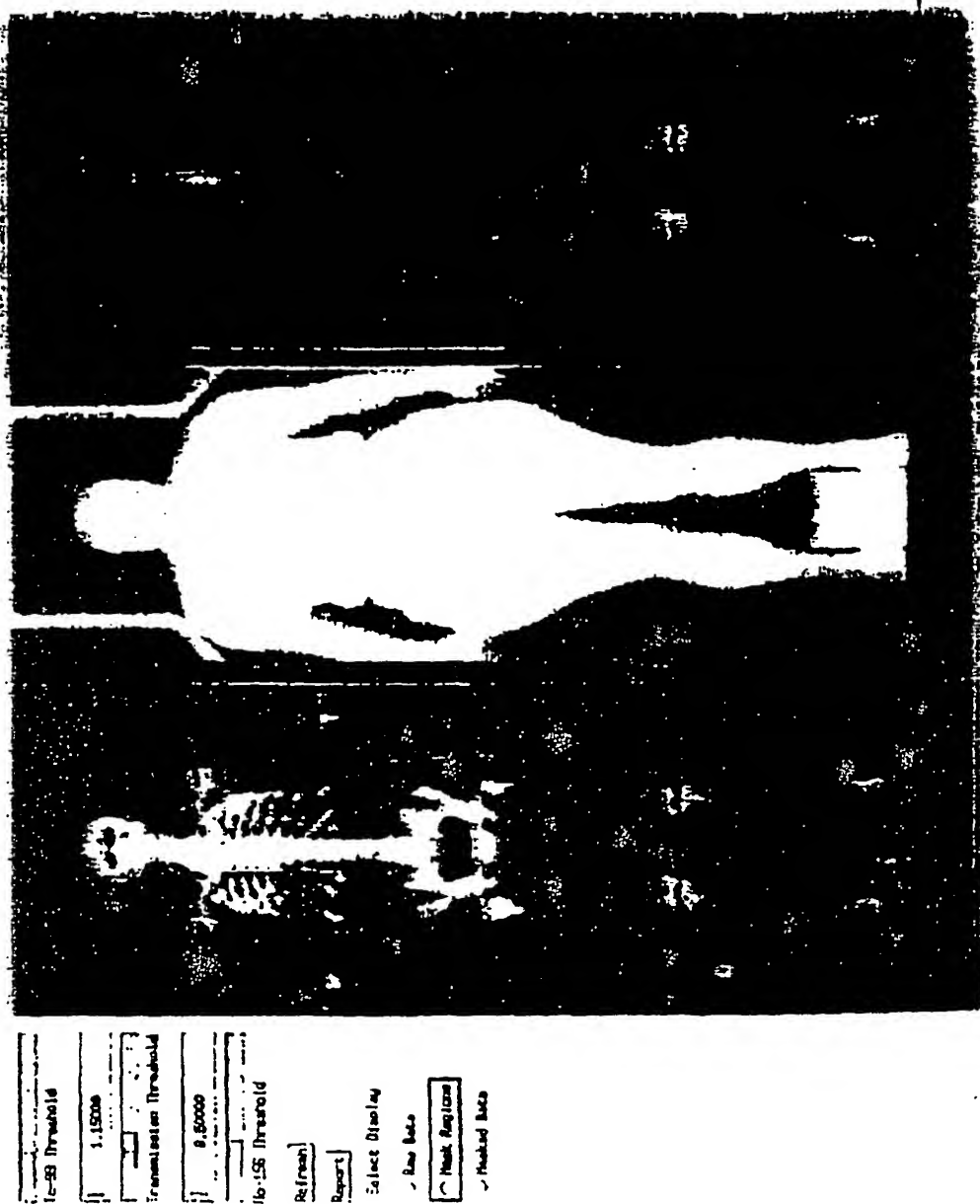


FIG. 4

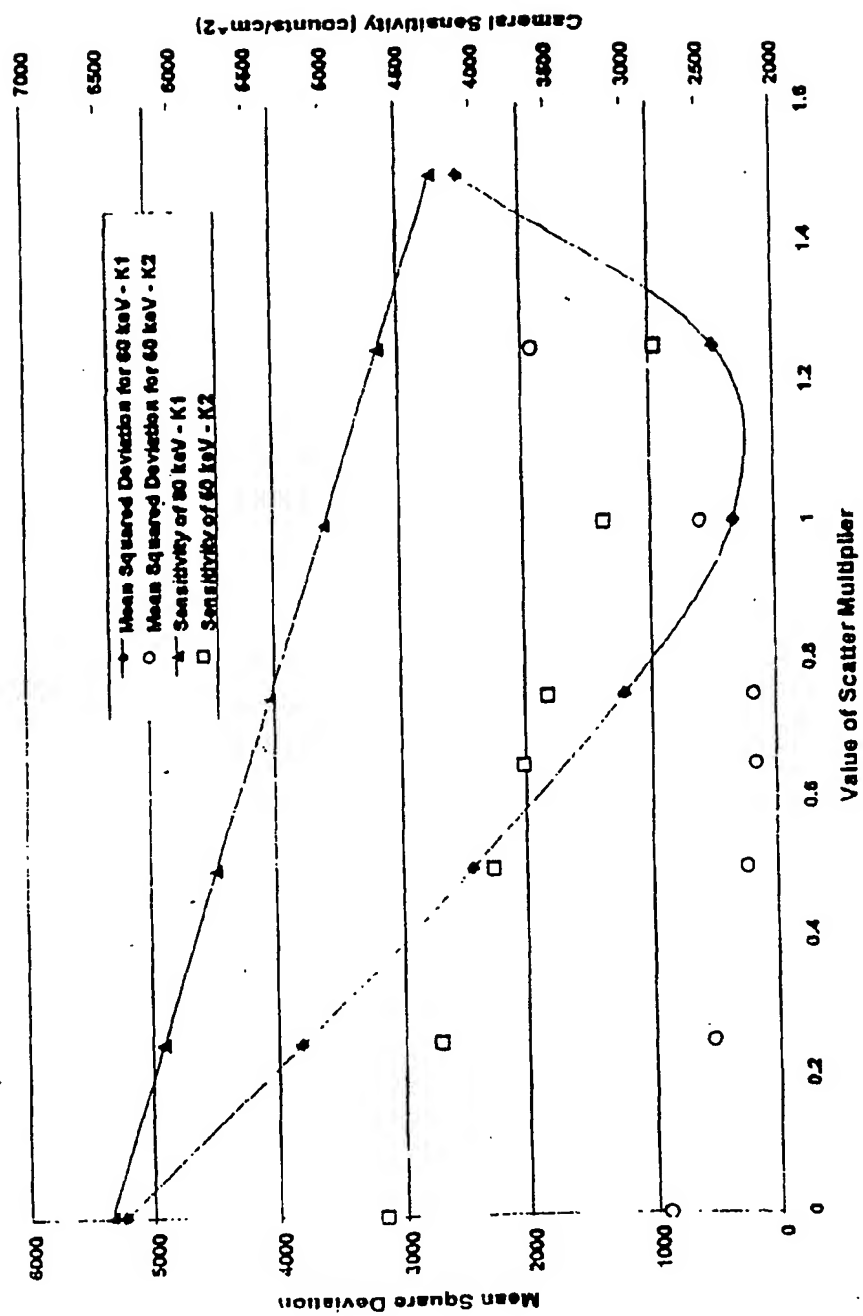


FIG. 5

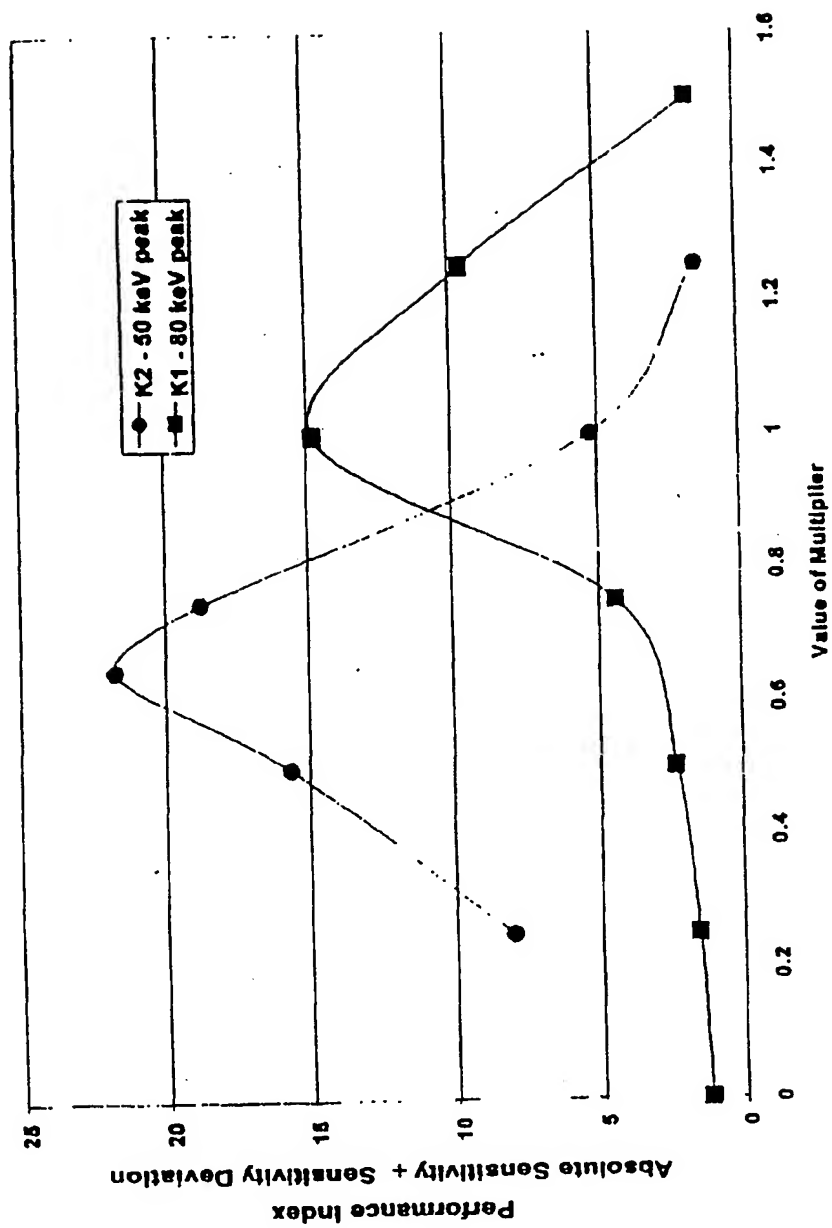


FIG. 6A

ACF Relationships for Co-57 & Ho-166 (80 keV)

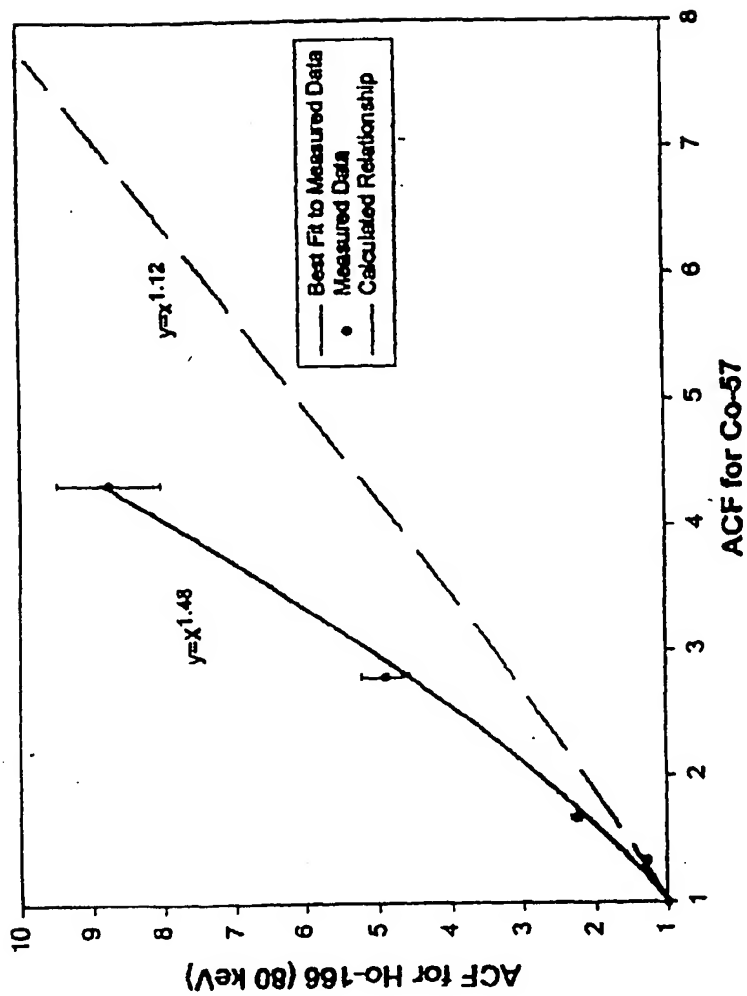


FIG. 6B

ACF Relationships for Co-57 &amp; Ho-166 (50 keV)

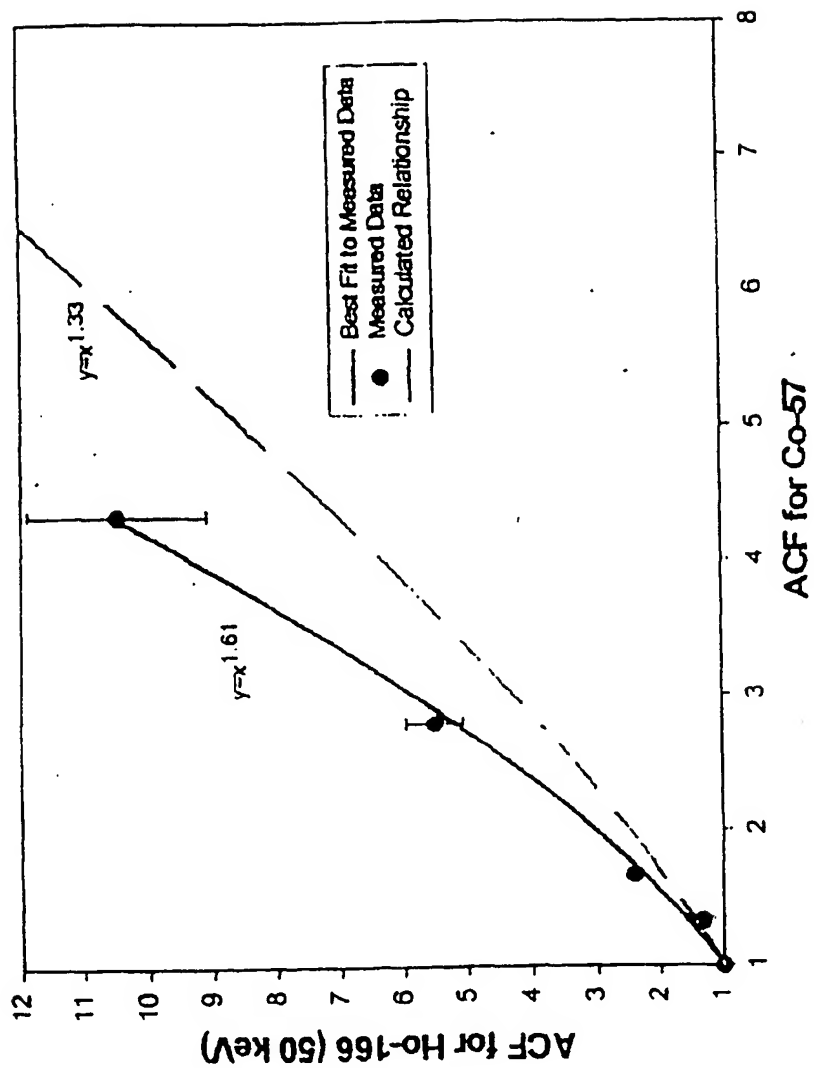


FIG. 7

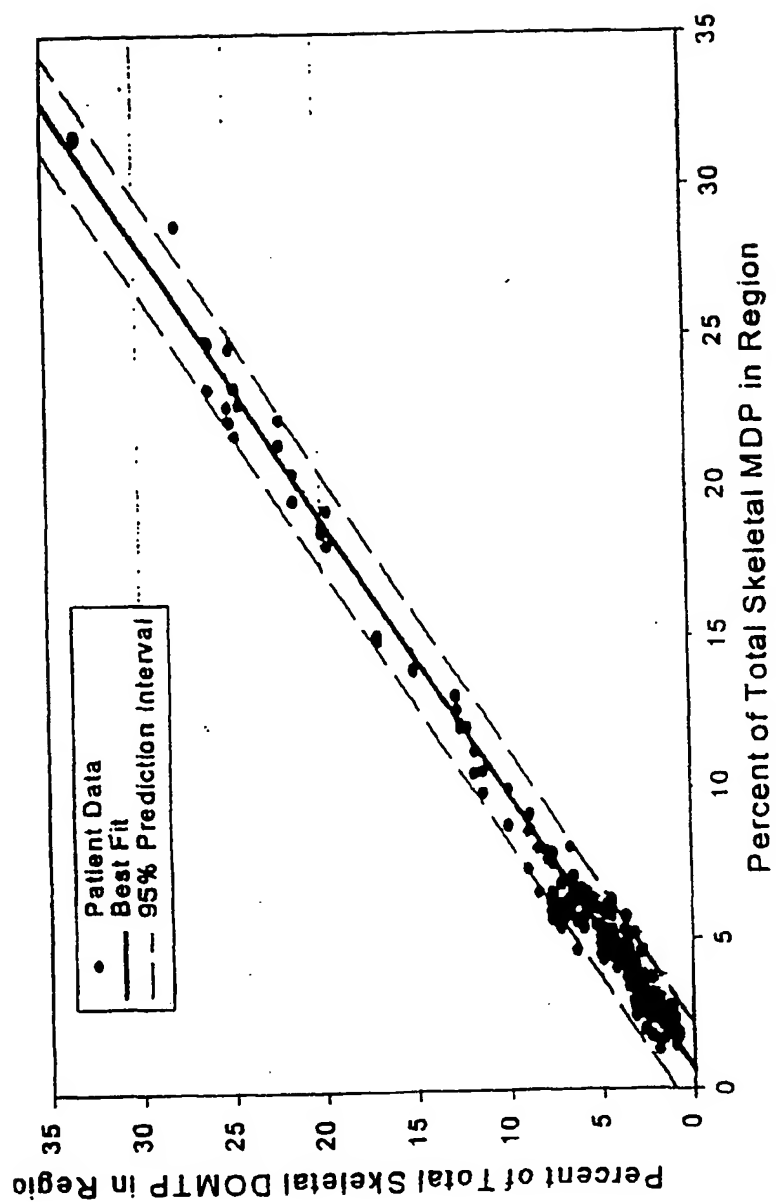


FIG. 8

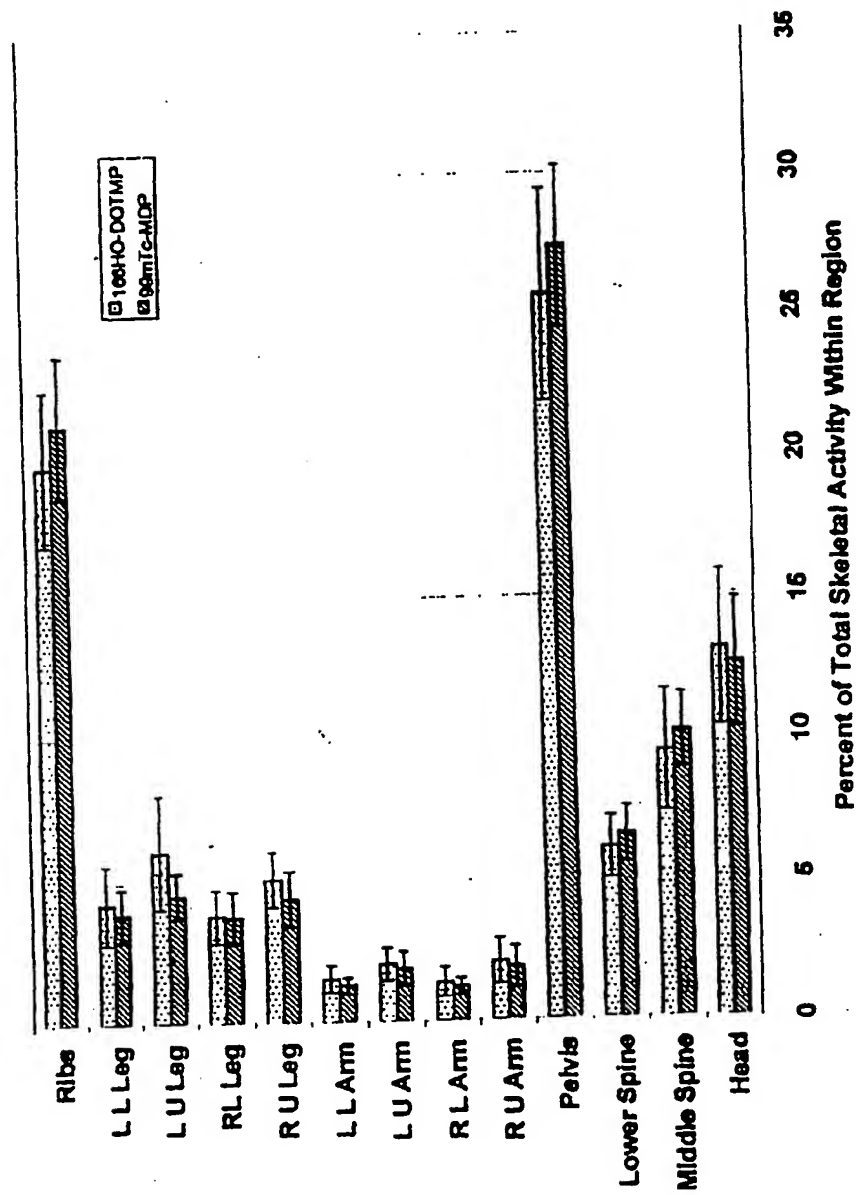




FIG. 9

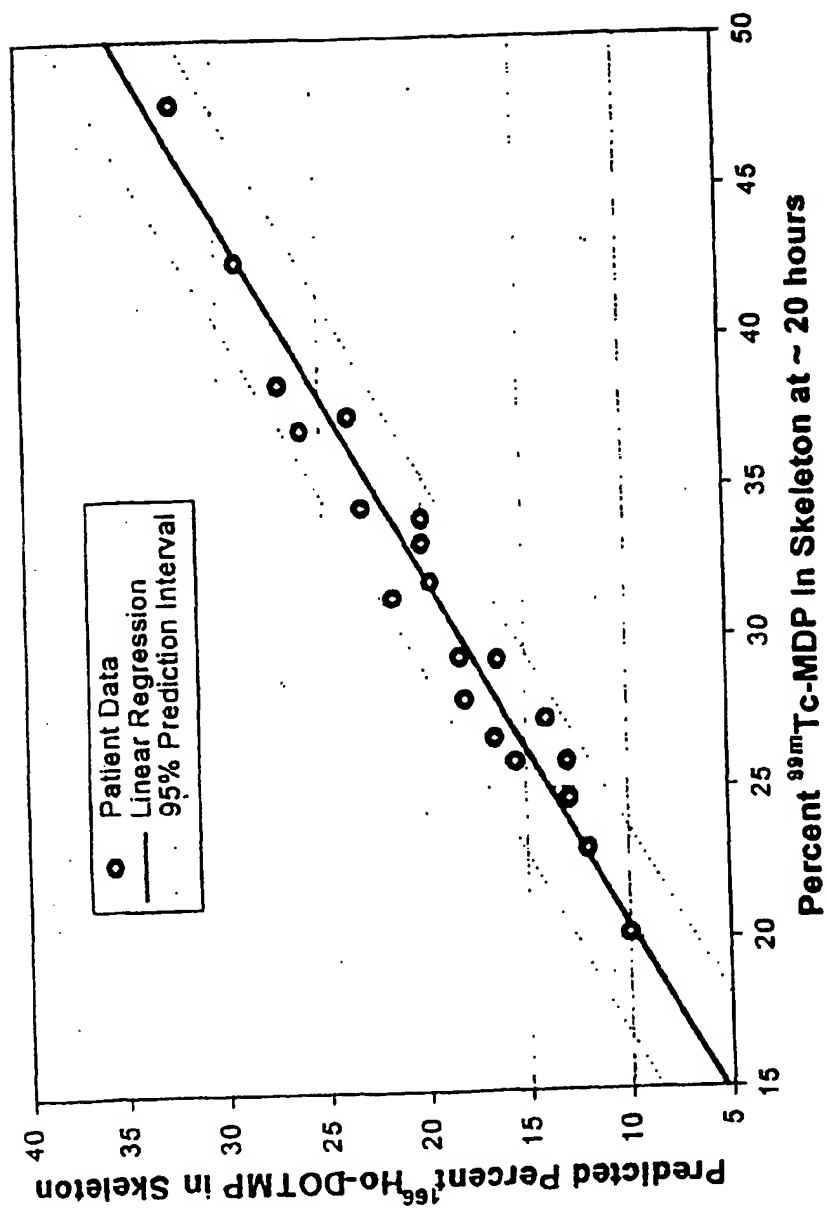


FIG. 10

